High temperature single crystal x-ray diffraction: structure of cubic manganese iodine and manganese bromine boracites

Crottaz, Olivier; Kubel, Frank; Schmid, Hans

How to cite

CROTTAZ, Olivier, KUBEL, Frank, SCHMID, Hans. High temperature single crystal x-ray diffraction: structure of cubic manganese iodine and manganese bromine boracites. In: Journal of solid state chemistry, 1995, vol. 120, n° 1, p. 60–63. doi: 10.1006/jssc.1995.1376

This publication URL: https://archive-ouverte.unige.ch/unige:31185

Publication DOI: 10.1006/jssc.1995.1376

JOURNAL OF SOLID STATE CHEMISTRY 120, 60–63 (1995)

High Temperature Single Crystal X-Ray Diffraction: Structure of Cubic Manganese Iodine and Manganese Bromine Boracites

O. Crottaz,[1] F. Kubel, and H. Schmid

Department of Mineral, Analytical, and Applied Chemistry, University of Geneva, 30 quai E. Ansermet, 1211 Geneva 4, Switzerland

Received March 31, 1995; in revised form June 19, 1995; accepted June 20, 1995

The structural parameters of optically controlled cubic manganese iodine boracite, $Mn_3B_7O_{13}I$, and manganese bromine boracite, $Mn_3B_7O_{13}Br$, have been refined on single crystals at 421 and 580 K, respectively (space group $F\bar{4}3c$, $Z = 8$). In order to perform these measurements, a low-cost heating device, based on a soldering iron heating element, has been used. Cell parameters were found to be 12.3404(3) Å for manganese iodine boracite and 12.3100(9) Å for manganese bromine boracite. The cell parameters and the deviation from planarity of the oxygen environment around the metal ion are found to be greater in manganese boracites than in other known cubic boracites.

1. INTRODUCTION

Boracites of chemical composition $M_3B_7O_{13}X$ (hereafter M–X, where M stands for a bivalent metal ion and X for a halogen ion) tend to undergo first order structural phase transitions from a high-temperature cubic structure (point group $\bar{4}3m$, non-centrosymmetric space group $F\bar{4}3c$) to noncubic low-temperature structures ($mm2$, m, $3m$, $\bar{4}2m$). In order to study these transitions, structural data of cubic boracites are required. The chemical environment of the metal ions in cubic boracites is shown in Fig. 1. The metal atoms are surrounded by four nearby oxygen atoms (O(1)) which are nearly coplanar and two more distant halogen atoms located on an axis perpendicular to the ideal M–O(1) plane. This region of the structure is supposed to be responsible for the phase transitions (see Ref. (1)) and can be described as an elongated octahedral environment of the metal ion with a tendency to a tetrahedral arrangement of the four nearly coplanar oxygen(1) ions (i.e., an octahedral environment with a tetragonal and a small tetrahedral deformation). The deformation of the oxygen plane varies with the metal and the halogen atoms present in the boracites. The deviation from planarity was introduced in the form of a parameter ε (defined as $\varepsilon(\text{Å}) = x(\text{O}(1)) \times a(\text{Å})$ by Nelmes (2). This parameter is related to the magnitude of the planar to tetragonal deformation of the oxygen ion arrangement and is more easily calculated than the "out of planarity" angle (that is, the angle between the ideal metal plane and the O(1) ions). To obtain correct results it is helpful to standardize the structures using the "structure tidy" program (3). However, it should be noted that the numerations of the oxygen and boron atoms are opposite to nonstandardized atomic positions published previously.

So far the cubic phase has been characterized for boracites with Mg, Cr, Fe, Co, Ni, Cu, and Zn as the M^{2+} ion [see (4) and Ref. therein, (5) for Fe–I, and (6) for Zn–Cl]. Except for Mg^{2+} and Zn^{2+} all these ions may present a Jahn–Teller effect, either in octahedral or in tetrahedral environment (7), which may make the understanding of the deformation difficult. Since Mn^{2+} is a $3d^5$ ion, where no Jahn–Teller effect is expected in the ground state for octahedral or tetrahedral coordination, a study of the cubic phase of boracites with manganese(II) may allow a better understanding of the cubic structures of boracites and of the cubic-orthorhombic phase-transition temperatures in the boracites. Consequently, we have chosen to refine the cubic structures of Mn–I and Mn–Br boracites.

2. EXPERIMENTAL

2.1. Apparatus

The data collections were made on a CAD-4 diffractometer.

For Mn–I and Mn–Br, the temperatures of the $mm2 \Rightarrow \bar{4}3m$ phase transitions are 407 and 543 K, respectively (8). In order to perform X-ray data collections, an optical control device and a low cost heating device, allowing single crystal studies in the range 320–520 K, have been developed.

The optical control device is needed to assure that the crystal is in the cubic and optically isotropic phase. This attachment consists of a polarizer, an analyzer, and a micro-

[1] To whom correspondence should be addressed.

0022-4596/95 $12.00

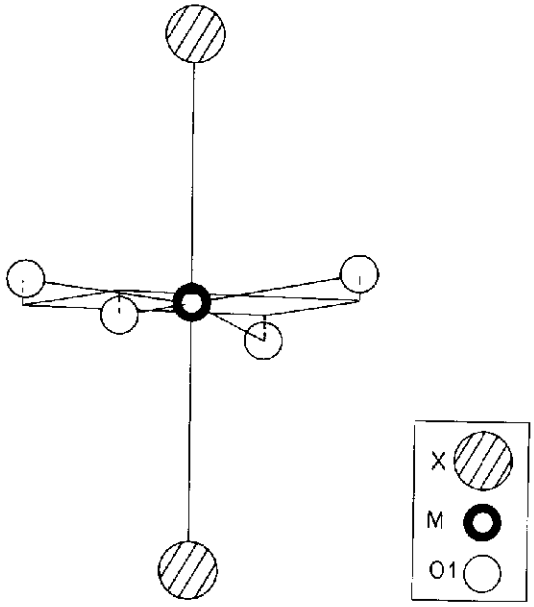

FIG. 1. Environment of the metal ions in cubic boracites.

scope. The crystal can be observed *in situ* in transmitted light, during heating.

The heating device consists of the heating element of a soldering iron (ϕ = 4.5 mm, P = 20 W) which is introduced into a T Pyrex tube (ϕ = 5.0 mm). The tube is insulated by Al foils. The soldering iron was connected to a variable voltage generator set to 3 V for Mn–I and to 6 V for Mn–Br. An air stream is introduced laterally into the T Pyrex tube. The air stream is provided by a compressed air system connected to a pressure reducer and a Porter flux regulator system. The flow rate was set to 9 liter/min. A sketch of this system is shown in Fig. 2. The temperature was measured with a Pt–Pt/Rh thermocouple, placed at

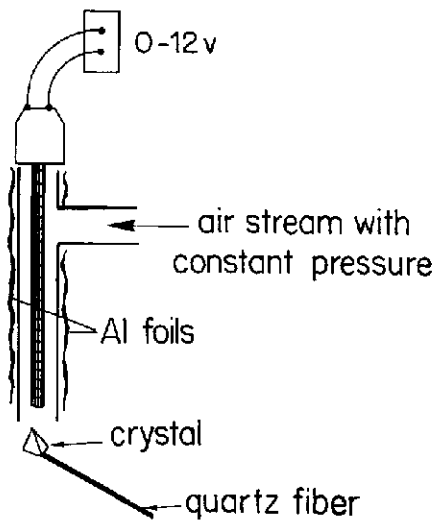

FIG. 2. Schematic sketch of the heating device used for the X-ray measurements at 421 ± 1 and 580 ± 5 K.

the site of the crystal, before and after the data collection. The temperature was set to 421 ± 1 K for Mn–I and 580 ± 5 K for Mn–Br. The crystals were fixed with standard Araldit glue on quartz fibers.

2.2. *Data Collection and Refinement*

Mn–I: bright pink dodecahedral crystal (ϕ = 0.1 mm) obtained by chemical vapor transport (9). Lattice parameter a = 12.3403(3) Å and V = 1879.29(5) Å^3 at 421 ± 1 K. CAD-4 automatic four-circle diffractometer, λ(Cu $K\alpha$) = 1.5418 Å, Z = 8, graphite monochromator, a complete sphere measured with $-15 < h < 15$, $-15 < k < 15$, $-15 < l < 15$, $[(\sin\theta)/\lambda]_{max}$ = 0.606 Å^{-1}, 3768 integrated intensities, $\omega - 2\theta$ scan, 2 standard reflections, maximum intensity change 6%, spherical absorption correction (μR = 0.59), lattice parameters determined from 24 reflections with $44° < 2\theta < 70°$; structure refinement by full-matrix least squares, function minimized $\Sigma w(|F_o| - |F_c|)^2$, unit weights; scattering factors for neutral atoms and anomalous-dispersion correction (*International Tables for X-ray Crystallography*, 1974, Vol. IV), 20 parameters refined [one scale factor, 4 positional parameters, 3 isotropic, 9 anisotropic, and one overall displacement parameters, one extinction parameter and one absolute structure parameter (10)], using the XTAL 3.2 program system (11). $(\Delta/\sigma)_{max} = 3 \times 10^{-4}$. The refined value for the absolute structure parameter was 0.025(25). A value close to 0 or 1 was expected for a cubic single crystal, as long as it is not mimetically twinned. Final R values are R = 2.0% and R_w = 2.7% for 99 contributing reflections.

Two measurements were made for Mn–Br: During a first attempt a data set was collected on a crystal which was mimetically twinned in the cubic phase due to growth twins. This type of twin (see, e.g., Fig. 16 in Ref. (12)) cannot be analyzed optically. The refinement allowed the calculation of an absolute structure parameter of 0.58(3) with R = 5.2% and R_w = 4.9%. The second measurement was made on a single crystal which was not twinned in the cubic phase.

Conditions for data collection were the same as for Mn–I, except: bright pink dodecahedral crystal (ϕ = 0.3 mm) with lattice parameter a = 12.3100(9) Å and V = 1865.4(4) Å^3 at 580 ± 5 K. $-15 < h, k < 15$, $-5 < l < 5$, $[(\sin\theta)/\lambda]_{max}$ = 0.634 Å^{-1}, 1478 integrated intensities, $\omega - 2\theta$ scan, 2 standard reflections, maximum intensity change 5%, spherical absorption correction (μR = 0.39), lattice parameters determined from 25 reflections with $32° < 2\theta < 86°$. $(\Delta/\sigma)_{max} = 0.5 \times 10^{-4}$. The refined value for the absolute structure parameter was −0.0018(2). Final R values are R = 3.7% and R_w = 4.8% for 90 contributing reflections.

The standardized atomic coordinates of Mn–I and Mn–Br are listed in Table 1.

TABLE 1
Standardized Fractional Atomic Coordinates and Equivalent Isotropic Displacement Parameters (Å² × 10²) of Mn–I and Mn–Br Boracites

Atom	Wyckoff notation	x	y	z	U_{eq}[a]
Mn–I (421 ± 1 K): a = 12.3404(3) Å					
Mn	24(*c*)	0	0.25	0.25	1.07(4)
I	8(*b*)	0.25	0.25	0.25	0.83(4)
B(1)	32(*e*)	0.0797(4)	0.0797(4)	0.0797(4)	0.9(1)
B(2)	24(*d*)	0.25	0	0	0.1(3)
O(1)	96(*h*)	0.0230(1)	0.0942(1)	0.1807(1)	0.41(5)
O(2)	8(*a*)	0	0	0	1.0(2)
Mn–Br (580 ± 5 K): a = 12.3100(9) Å					
Mn	24(*c*)	0	0.25	0.25	3.23(7)
Br	8(*b*)	0.25	0.25	0.25	2.47(8)
B(1)	32(*e*)	0.0814(5)	0.0814(5)	0.0814(5)	2.0(2)
B(2)	24(*d*)	0.25	0	0	1.2(4)
O(1)	96(*h*)	0.0234(2)	0.0950(2)	0.1814(2)	1.1(7)
O(2)	8(*a*)	0	0	0	2.1(2)

[a] U_{eq} is defined as one-third of the trace of the orthogonalized U_{ij} tensor.

3. RESULTS AND DISCUSSION

The main interatomic distances in cubic iodine and bromine boracites are presented in Table 2. The last line (i.e., Δl_{max}) shows the difference between extreme values. It can be noted that there is a significant change of the M–X, M–O(1), and B(1)–O(2) bond distances when metals and halogens are varied. Other distances like the O(1)–O(1), B(1)–O(1) and B(2)–O(1) are not influenced. Except for the tetrahedrally coordinated B(1) atoms the boron–oxygen distances show only little change with the type of boracite and temperature, thus confirming the picture of a rigid boron–oxygen network. Due to this rigidity considerable modifications may mainly be expected in the metal environment which therefore is discussed in detail.

The Mn–O(1) and Mn–X bonds are longer in Mn–I and Mn–Br than any other metal–oxygen(1) or metal–halogen bond in the other known cubic boracites, as reflected by the larger unit cell parameters of these compounds. The out of planarity angles are equal to 7.68(1)° in Mn–I and 7.85(3)° in Mn–Br while the deviation from planarity parameters (ε) are 0.2834(12) Å in Mn–I and 0.2881(24) Å in Mn–Br. Similarly to other cubic boracites, the metal ion vibrates mainly in the direction parallel to the weak metal halogen bond [$\langle u\rangle_{\parallel}^2/\langle u\rangle_{\perp}^2$ = 3.9(2) in Mn–I and 5.2(4) in Mn–Br] rather than in the direction of the strong metal–oxygen bonds. The values obtained for the [$\langle u\rangle_{\parallel}^2/\langle u\rangle_{\perp}^2$ ratios are in agreement with those of other boracites, found to be between 2.7(3) for Cr–I and 5.1(3) for Cr–Cl [see Ref. (4)].

The deviation from planarity of the MO_4 group, ε, as a function of the cubic cell parameters is shown in Fig. 3. The overall trend of ε to increase with the cell parameter, as suggested by Monnier *et al.* (13), is respected as Mn–I and Mn–Br show greater deformations than other boracites. It can be noted that the Zn–Cl boracite does not follow the general trend as it is much more planar than expected by the value of the lattice parameter. This may be due to the d^{10} configuration of the Zn^{2+} atoms. The fact that extreme values are observed for boracites with Zn^{2+} (d^{10}) and Mn^{2+} (d^5) is another indication of the importance of the electronic configuration of the transition metal on the structure of cubic boracites.

When the ε parameter is plotted as a function of the M–O(1) bond length it appears that the largest ε corresponds to the longest M–O(1) bond. But if the geometry around the M ions is governed mainly by sterical effects, the largest ε should correspond to the shortest M–O(1) bond. This suggests that, as the M–O(1) distance gets shorter, the bond strength increases, thus leading to a more planar environment. This effect may be in relation with the sp^2 hybridization of the O(1) ions which may lead to an interaction between the M^{2+} empty 4*d* shell and the O(1) electron lone pair. This interaction could tend to

TABLE 2
Interatomic Distances (Å) in Cubic Mn–Br, Mn–I, and in Other Cubic Iodine Boracites

Name	M–X	M–O(1)	O(1)–O(1)shortest	B(1)–O(1)	B(2)-O(1)	B(1)–O(2)	Ref.
Cr–I	3.0520(2)	2.075(2)	2.393(2)	1.439(3)	1.479(2)	1.682(2)	(13)
Fe–I (373 K)	3.06	2.10	~2.3	~1.5	~1.4	~1.5	(6)
Co–I	3.030(1)	2.056(2)	2.390(2)	1.434(3)	1.463(1)	1.673(3)	(14)
Ni–I	3.011(1)	2.053(3)	2.390(4)	1.433(4)	1.465(3)	1.673(5)	(15)
Cu–I	3.005(1)	2.008(4)	2.389(5)	1.431(8)	1.469(4)	1.692(7)	(16)
Mn–I (471 K)	**3.0851(1)**	**2.1233(12)**	**2.3872(17)**	**1.441(5)**	**1.4708(12)**	**1.703(5)**	
Mn–Br (580 K)	**3.0775(2)**	**2.107(2)**	**2.386(4)**	**1.433(7)**	**1.471(3)**	**1.736(6)**	
Δl_{max} (without Fe–I)	0.0801(2)	0.115(5)	0.006(3)	0.010(13)	0.016(3)	0.063(11)	

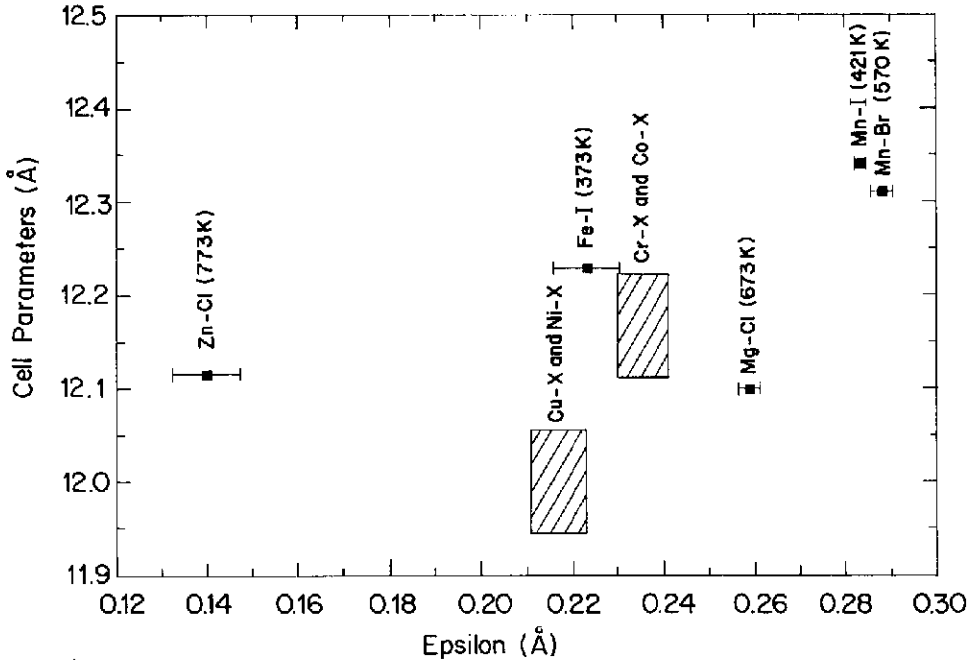

FIG. 3. Deviation from planarity, ε (for definition see text), of the O-atom environment around the metal atoms (site symmetry of metal atoms $\bar{4}$) in cubic boracites as a function of cubic cell parameter, a. Data include Refs. (4–6 and 13–20). Error bars ∓ 1 e.s.d. Dashed regions include (i) Ni–I (77 and 293 K), Cu–Cl (390 K), Cu–Br, and Cu–I and (ii) Cr–Cl, Cr–Br (113 and 293 K), Cr–I, and Co–I. See Ref. (3) for details.

preserve a planar environment. This hypothesis can also help to explain the great difference of planarity between the Mg–Cl and Zn–Cl boracites, as the interaction between the oxygen lone pairs and the empty d shell are weaker in Mg–Cl ($3d$ shell) than in Zn–Cl ($4d$ shell).

More theoretical studies are necessary in order to understand the effect of the electronic configuration of the metal ions on the structure of cubic boracites. The possible interactions between the metal ions and the sp^2 O(1) ions also remain unclear.

ACKNOWLEDGMENT

The authors are grateful for the support of the Swiss National Science Foundation.

REFERENCES

1. F. Kubel and A. M. Janner, *Acta Crystallogr., Sect. C* **49,** 657 (1993).
2. R. J. Nelmes, *J. Phys. C* **7,** 3855 (1974).
3. L. M. Gelato and E. Parthé, *J. Appl. Crystallogr.* **20,** 139 (1987).
4. M. Yoshida, K. Yvon, F. Kubel, and H. Schmid, *Acta Crystallogr., Sect. B* **48,** 30 (1992).
5. F. Kubel, *Ferroelectrics* **160,** 61 (1994).
6. F. Kubel, submitted for publication.
7. J. D. Dunitz and L. E. Orgel, *J. Phys. Chem. Solids* **3,** 20 (1957).
8. H. Schmid and H. Tippmann, *Ferroelectrics* **20,** 21 (1978).
9. H. Schmid, *J. Phys. Chem. Solids* **26,** 973 (1965).
10. H. D. Flack, *Acta Crystallogr., Sect. A* **39,** 876 (1983).
11. S. R. Hall, H. D. Flack, and J. M. Stewart (Eds.), "XTAL3.2 Reference Manual." Universities of Western Australia, Geneva, and Maryland, 1992.
12. H. Schmid, *Rost Krist.* **7,** 32 (1967); [*Growth Crystals (Engl. Transl.)* **7,** 25 (1969)].
13. A. Monnier, G. Berset, H. Schmid, and K. Yvon, *Acta Crystallogr., Sect. C* **43,** 1243 (1987).
14. R. J. Nelmes and W. J. Hay, *J. Phys. C* **14,** 5247 (1981).
15. R. J. Nelmes and F. R. Thornley, *J. Phys. C* **9,** 665 (1976).
16. G. Berset, W. Depmeier, R. Boutellier, and H. Schmid, *Acta Crystallogr., Sect. C* **41,** 1694 (1985).
17. F. R. Thornley, N. S. J. Kennedy, and R. J. Nelmes, *J. Phys. C* **9,** 681 (1976).
18. F. R. Thornley, R. J. Nelmes, and N. S. J. Kennedy, *Ferroelectrics* **13,** 357 (1976).
19. R. J. Nelmes and F. R. Thornley, *J. Phys. C* **7,** 3855 (1974).
20. S. Sueno, J. R. Clark, J. J. Papike, and J. A. Konnert, *Am. Miner.* **58,** 691 (1973).